The crust and mantle of Mars

Maria T. Zuber

Department of Earth, Atmospheric and Planetary Sciences, Massachusetts Institute of Technology, Cambridge, Massachusetts 02139-4307, USA (e-mail: zuber@mit.edu)

Clues to the history of Mars are recorded in the chemistry and structure of the planet's crust and mantle. The mantle is the rocky, interior region of the planet that transports heat generated during accretion and subsequent core formation. The crust formed by melting of the upper mantle, and has been shaped and re-distributed by impact, volcanism, mantle flow and erosion. Observations point to a dynamically active interior in the early phases of martian history, followed by a rapid fall-off in heat transport that significantly influenced the geological, geophysical and geochemical evolution of the planet, including the history of water and climate.

The different geological evolution of Mars compared to Earth is to due primarily to Mars' smaller size. The radius of Mars is about half that of Earth, and so Mars probably heated up and cooled off more quickly. Thus, geological activity manifest as tectonism, volcanism and the associated release of volatiles should have occurred relatively earlier for Mars than for Earth. On Earth, convective cooling of the interior drives the motions of surface plates and is accompanied by the creation of seafloor at mid-ocean ridges and consumption of plates at subduction zones. In contrast, Mars is currently a single-plate planet with a thick, rigid outer shell. But it is possible that earlier in martian history, when internal heat loss was more intense, the planet displayed thinner and possibly even mobile plates[1].

Understanding the evolution of the crust and mantle of Mars has been aided significantly by orbital global geophysical measurements of topography, gravity and magnetics, Earth-based and orbital spectra, orbital- and lander-scale images of the surface, and geochemical measurements of martian meteorites. These data collectively tell the story of an early, dynamic martian interior.

Composition of crust and mantle

Crustal composition

Information on the composition of the crust of Mars has been obtained from Earth-based[2] and orbital spectra[3–6], *in situ* spectral and chemical observations from the Viking and Pathfinder landers[7], and geochemical analyses of meteorites believed to have come from Mars[8,9]. The surface is composed of a mixture of relatively pristine igneous rocks overlain by highly oxidized weathering products that constitute the relatively bright dust and soils. The reddish colour of the martian surface is due to the presence of ferric iron-bearing minerals in the oxidized surface layer[10,11]. At the local scale, the Viking landers revealed the likely presence of peroxide, a reactive oxidant. The surface sampled *in situ* lacks organic compounds, which, although periodically replenished by meteorites, are probably destroyed by the oxidants as well as intense ultraviolet radiation. If early Mars once had a significantly denser atmosphere than present (ref. 12, and see review in this issue by Jakosky and Phillips, pages 237–244), then evidence should be preserved in the crustal surface layer as carbonates and sulphates. Limited amounts of both have been found in martian meteorites[9], and sulphates have been found *in situ*[13], but neither has been detected conclusively from remote spectral data, which are sensitive at levels of 5–10% abundance[14,15].

Thermal-emission spectrometer data from the Mars Global Surveyor (MGS) orbiter suggest that dark regions exhibit two compositions[6]: a basalt-rich component in the southern highlands and andesite-rich component in the northern lowlands. On Earth, basalt is a common volcanic rock formed by melting of the upper mantle, while andesite is found almost exclusively in subduction zone environments, where water has been important in the melt generation process. Andesite formed by fractional crystallization of dry basaltic magma would require large amounts of melting[7], but for water-rich magmas a greater proportion of andesitic magma can be produced[16,17]. An alternative interpretation is that the proposed andesite spectral features reflect a basaltic composition with a significant glass component[18].

Certain classes of basaltic achondrite meteorites — shergottites, nakhilites and chassignites (collectively termed SNCs) — are believed to have been ejected from the martian surface by one or more impacts[19] within the past 1–20 million years (Myr). Evidence for a martian origin of these meteorites includes relatively young crystallization ages (0.15 to 1.3 billion years (Gyr)) by terrestrial planet standards[19–21], and the presence of trapped gases that match isotopically the martian atmosphere[22–25]. Geochemical analyses indicate that all the martian meteorites are picritic or basaltic lavas or were derived from basaltic magmas[7], which is consistent with visual and near-infrared spectral observations[5], but not thermal-infrared orbital

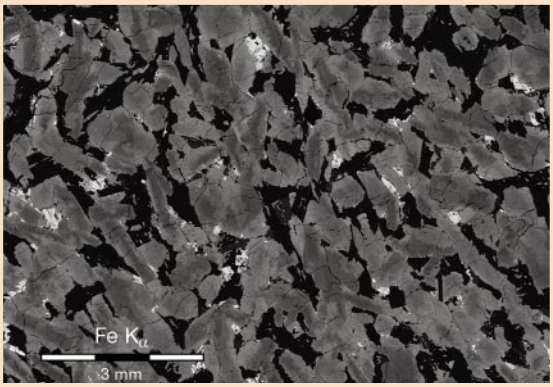

Figure 1 Photograph of a microscopic thin section of the Shergotty meteorite, which is believed to represent a sample of the martian crust.

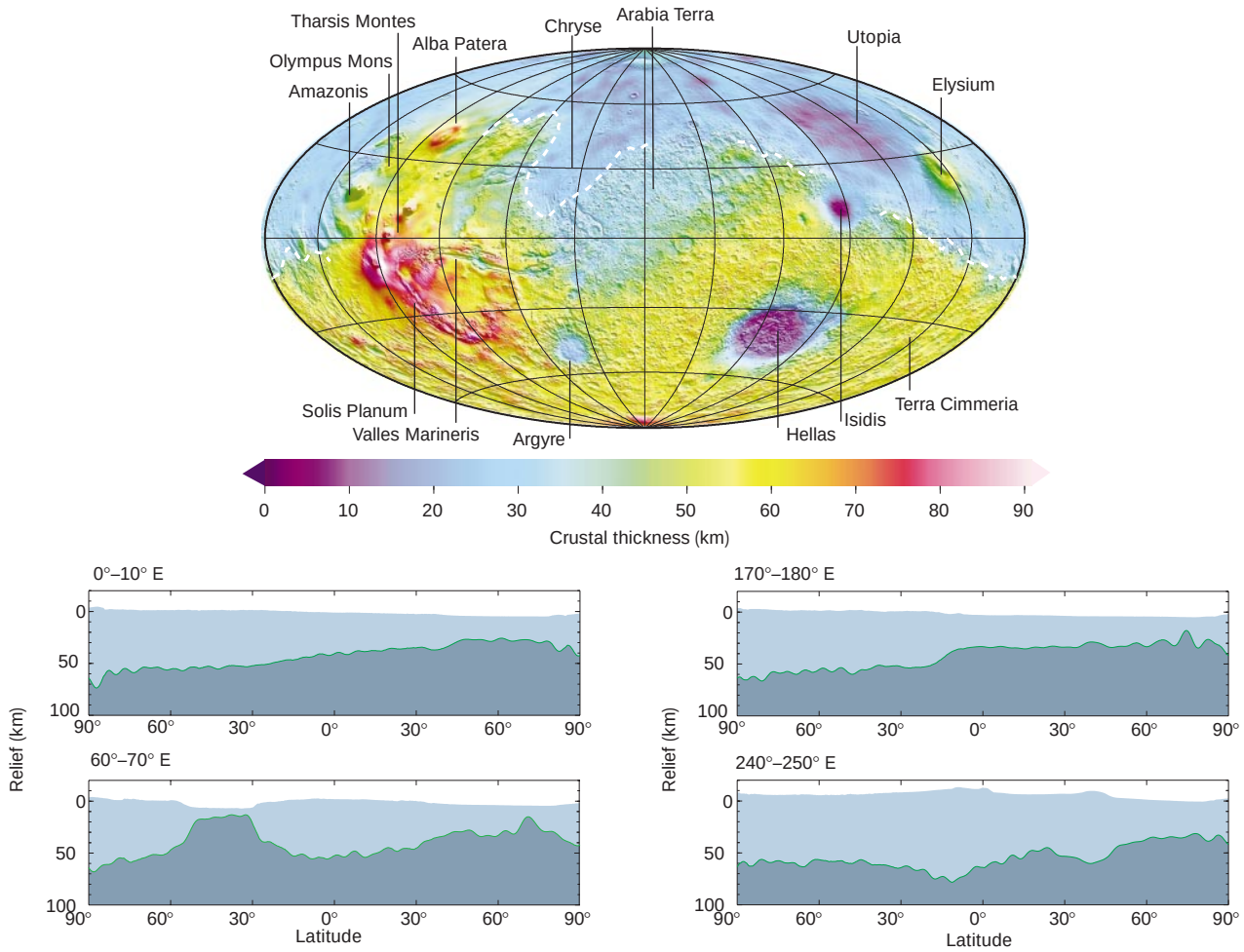

Figure 2 The crustal thickness of Mars assuming a constant-density crust and mantle. The model (crust1004), shown over a shaded relief map, is based on Mars Global Surveyor gravity[55] and topography[54] fields. The crustal thickness model has a spatial resolution of ~180 km. The map projection is Molleweide and the coordinate system is areocentric with an east-positive longitude convention. The dashed line shows the location of the geological dichotomy boundary between the northern and southern hemispheres. The boundary is plotted only where it is distinctively expressed. Note that the crustal provinces of the northern and southern hemisphere follow the yellow-green interface and do not correlate everywhere with the surficial expression of the geological dichotomy. Also shown are 10°-averaged south pole-to-north pole longitudinal transects of crustal structure, where light grey corresponds to crust and dark grey corresponds to mantle. The transects for longitudes 0°–10° E and 170°–180° E show crustal provinces of the northern and southern hemisphere. The transect through 60°–70° E shows crustal thinning beneath the Hellas basin, and that through 250° E shows crustal thickening beneath Tharsis.

observations[6,15]. The parent magmas of the martian meteorites were probably generated by partial melting of the uppermost mantle of Mars and were emplaced at the surface and within the crust by volcanic and magmatic processes. The meteorite ALH84001, renowned for proposed evidence of past biological activity[26], has been traced to a martian origin by microscopic-scale textural features and its oxygen isotopic signature[27]. However, this meteorite has a crystallization age of ~4.5 Gyr and probably represents a sample of ancient crust[28–30]. Of the martian meteorites, the shergottites (Fig. 1) represent late-stage magmatic products that are considered the most representative samples of unmodified martian crust, but the parent rocks of all martian meteorites sample only a small part of the martian surface.

Mantle composition

Compositions of martian meteorites in combination with models of the planet's density distribution with depth inferred from geophysical constraints[31–33] lead to inferences about the composition of the martian mantle. It has been generally assumed that the bulk composition of Mars is 'chondritic', that is, approximating the composition of carbonaceous chondrite meteorites[34,35], which are believed to be representative of the most primitive material in the Solar System. It has been suggested that the bulk composition of Mars may deviate from carbonaceous chondrites[36] and, unlike the crust, might be characterized by reducing conditions[37]. A model of the martian interior based on martian meteorites[38] suggests that the planet was accreted from two chemically distinct components, the first of which was volatile-rich and oxidizing, and the second was reducing and consisted of high-temperature minerals. These components may have mixed to provide a mantle that is now chemically homogeneous[34].

Various bulk composition models of Mars have been proposed and a common feature is enrichment in iron relative to Earth's mantle. Such models can be converted to pressure- and temperature-dependent mineralogies. One plausible structure[35], based on the model of Dreibus and Wanke[34], has the upper martian mantle similar to Earth's, consisting primarily of the mineral olivine $[(Mg,Fe)_2SiO_4]$. With increasing depth a transition zone would consist of the more densely packed spinel structure (the high-pressure polymorph of olivine), and the lower mantle would contain a narrow zone rich in an even denser perovskite structure $[(Mg,Fe)SiO_3]$. Transitions to denser phases occur at greater depth in the martian

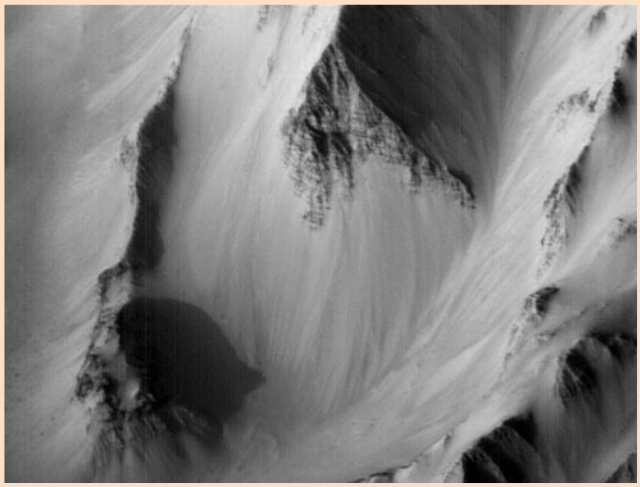

Figure 3 Mars Orbiter Camera image of layering in the western Tithonium Chasma/Ius Chasma region of the Valles Marineris, centred at 6.6° S, 269.6° E (ref. 64). The resolution is 6.45 m pixel^{-1} across by 9.65 m pixel^{-1} down.

mantle than on Earth because of the lower gravity. For example, the olivine–spinel transition that occurs at 400-km depth on Earth is expected at a depth of about 1,000 km on Mars. Whether or not the spinel–perovskite phase change actually occurs within the mantle depends on the mantle temperature and the size of the core. The moment of inertia factor determined from tracking the Pathfinder lander[33], in combination with estimates of core composition (ref. 39, and see review in this issue by Stevenson, pages 214–219), put the core–mantle boundary at a radial distance from Mars' centre of mass of 1,300–1,700 km.

Structure of the crust

Surface ages

Box 1 shows geological epochs on Mars, which, from oldest to youngest, are the Noachian, Hesperian and Amazonian, named after stratigraphic examples at type localities. Although it is possible to establish the relative timing of events during crustal evolution on the basis of stratigraphic superposition relationships[40] and globally distributed geophysical and geological observations[41], there is a significant uncertainty as to when events occurred in an absolute time frame, because the initial impact flux is unknown. A variety of observations point to the fact that the predominance of planet-scale events occurred during the earliest martian epoch, the Noachian (see reviews in this issue by Jakosky and Phillips (pages 237–244), Stevenson (pages 214–219) and Baker (pages 228–236)), consistent with the concept of an 'accelerated' martian thermal evolution compared to Earth.

Crustal physiography

The first impression of the martian crust is that it exhibits a much different appearance in the northern and southern hemispheres (Fig. 2). This hemispheric dichotomy[42,43] is manifest topographically as a contrast between the high-standing southern hemisphere and low-lying northern hemisphere, such that the south pole is nearly 6-km higher than the north pole[44,45]. The dichotomy is also expressed in the surface geology, as the southern-hemisphere crust is heavily cratered and thus ancient (Noachian in age). In contrast, the northern hemisphere is smoother and displays far fewer craters, reflecting the fact that it has been resurfaced later, during the Hesperian epoch[46,47]. The dashed line in Fig. 2 corresponds to the boundary between geologically older and younger provinces. The boundary zone is characterized by complex geology[48,49] and offsets in regional elevation[50].

Another prominent global-scale feature is Tharsis, a vast, complex topographic rise that is a locus of volcanic activity and includes the

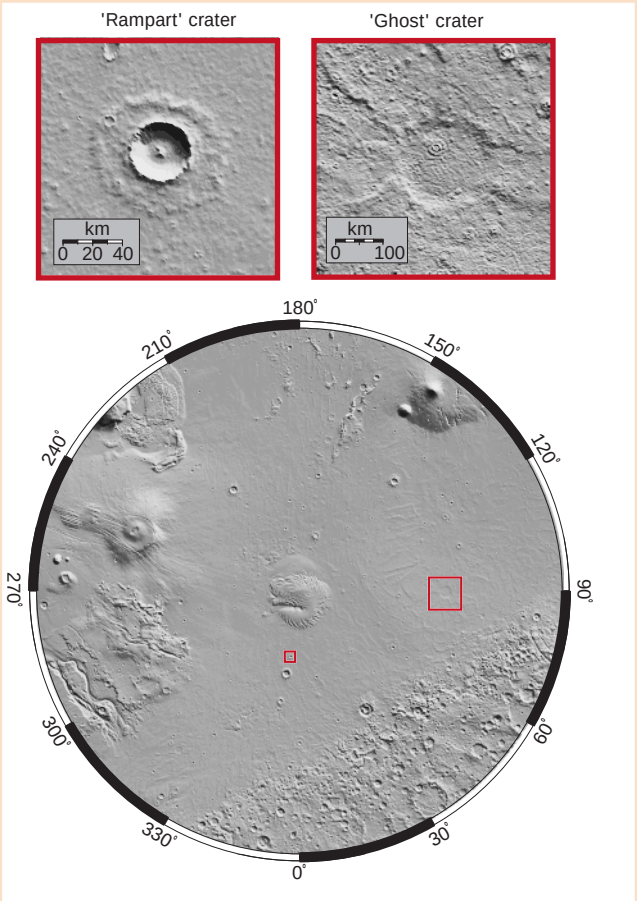

Figure 4 Shaded relief map centred on the north pole of Mars[121]. Insets show a 'rampart' crater whose unusual ejecta blanket represents evidence for the presence of subsurface volatiles at the time of the impact event, and a previously unrecognized, partially buried 'ghost' crater within the Utopia basin, which provides an estimate of the thickness of fill within Utopia since the buried crater formed.

largest martian shield volcanoes. The formation of Tharsis represented a principal source of stress in the martian crust and resulted in significant tectonism (fracturing and faulting), most prominently expressed by the massive Valles Marineris canyon system. The Elysium region in the northern lowlands is another crustal rise marked by volcanism and faulting, at a much smaller scale than Tharsis.

Mars also preserves the record of large impacts that occurred during the Noachian in the post-accretional phase of heavy bombardment. The largest preserved basins are Hellas, Utopia, Argyre and Isidis. The Utopia basin, buried beneath the plains of the northern hemisphere[51], is about the same size as Hellas, but much shallower (2.5 km compared with 11 km)[45], which provides evidence for assessing the thickness of the northern-hemisphere fill in that region.

Crustal structure

As a result of the recent availability of globally distributed, high-resolution topography[45] and gravity[52] data, it is now possible to map the subsurface structure of the martian crust and upper mantle[53]. Inversions for planetary internal structure from gravity and topography are inherently non-unique and should, whenever possible, be developed in concert with additional constraints. The simplest plausible structure assumes a uniform-density crust and mantle, which provides a lower limit on the planet's mean crustal thickness and global crustal volume, but does not account for density variations within the crust or upper mantle. Figure 2 shows a crustal thickness model that was constructed under this assumption from the most up-to-date topography[54] and gravity[55] fields from MGS[56]. The model

assumes a crustal density of 2,900 kg m^{-3}, consistent with plausible crustal compositions, and an assumed mantle density of 3,500 kg m^{-3}, consistent with bulk composition models[34]. The mean thickness of the crust in Fig. 2 is ~50 km, corresponding to 4.4% of the planetary volume.

Because of the absence of seismic measurements, the thickness of the martian crust cannot, as on the Earth and Moon, be 'anchored' by the depth of a seismic velocity discontinuity that characterizes the interface between layers of different compositions. Instead, the mean crustal thickness is constrained by calculations of the minimum value of viscosity of the lower crust that allows the observed relief at the crust–mantle boundary to be maintained over geological time[53,57]. Different assumptions about the density difference between the crust and mantle or the crustal rheology or thermal structure could lead to variations in mean crustal thickness of as much as several tens of per cent. But for any reasonable assumptions, the mean thickness is inconsistent with earlier studies[58] that suggested a thickness of 100–250 km. The earlier estimates were based on geophysical inversions of poor-quality data[59] and the observation that martian meteorites exhibit a composition consistent with significant partial melting, which was interpreted as indicative of a large crustal volume[58,60].

An alternative model could invoke a crust of approximately uniform thickness that exhibits spatial variations in crustal and/or mantle density. Although possible, such a scenario is not easily reconciled with the observed progressive change in crustal composition from the southern hemisphere to the north. For example, the 'pole-to-pole' variation in crustal thickness shown in Fig. 2 could instead be explained by a 2% difference in the density of the mantle distributed over a depth range of 300 km. However, a planetary-scale density variation would be difficult to maintain over geological time against mantle flow, particularly early in martian history subsequent to the emplacement of the crust when mantle temperatures were likely to have been high. A warm interior would enhance crustal flow and cause variations in crustal thickness to relax away by viscous flow.

Figure 2 shows that, as for the Moon[61,62], the martian crust is thinned beneath all resolvable major impact basins, owing to a combination of excavation and crustal rebound during the impact process. The Tharsis province is characterized by a complex thick crust, representing massive ($\sim 3 \times 10^8$ km^3) accumulation of magmatic and volcanic materials that point to volcanic construction as a significant contributor to its high-standing topography[53,63]. The crust beneath Valles Marineris, which cuts a deep crustal exposure through eastern Tharsis, is thinned along the central axis, as in terrestrial rift zones. The interpretation of Tharsis as a massive volcanic pile is strengthened by the probable recognition in Valles Marineris that the full vertical extent of the canyon walls are composed of layered volcanic sequences (Fig. 3)[64]. Both Elysium and the Solis Planum region in southern Tharsis appear as topographic rises with crustal roots that represent evidence of regionally enhanced melting.

Figure 2 also shows that Mars displays two crustal provinces that do not correlate entirely with the geological expression of the hemispheric dichotomy. One crustal province extends from the south polar region towards the north, and encompasses much of the southern highlands and the southern half of Tharsis. The second includes the northern lowlands and Arabia Terra. Although the boundary between crustal provinces correlates imperfectly with the boundary of the geological dichotomy, it does show some correlation with global-scale compositional units mapped by thermal emission observations[6]. On the basis of crustal structure, Arabia Terra may represent exposed basement of the resurfaced plains in the northern lowlands.

The northern lowlands

Before the launch of MGS, the northern lowlands had been viewed as vast, featureless plains, consisting of mainly Hesperian-aged volcanic flows[46,47,65]. But high-resolution shaded-relief topography (Fig. 4) now shows the lowlands to be rich in subtle detail, containing pervasive tectonic ridges[66,67], morphologic evidence for the flow of water far from the mouths of outflow channels[54], and 'ghost craters' that have been partially buried by plains material[68,69]. Gravity and topography data now suggest a significant sedimentary contribution to the northern-hemisphere resurfacing[53].

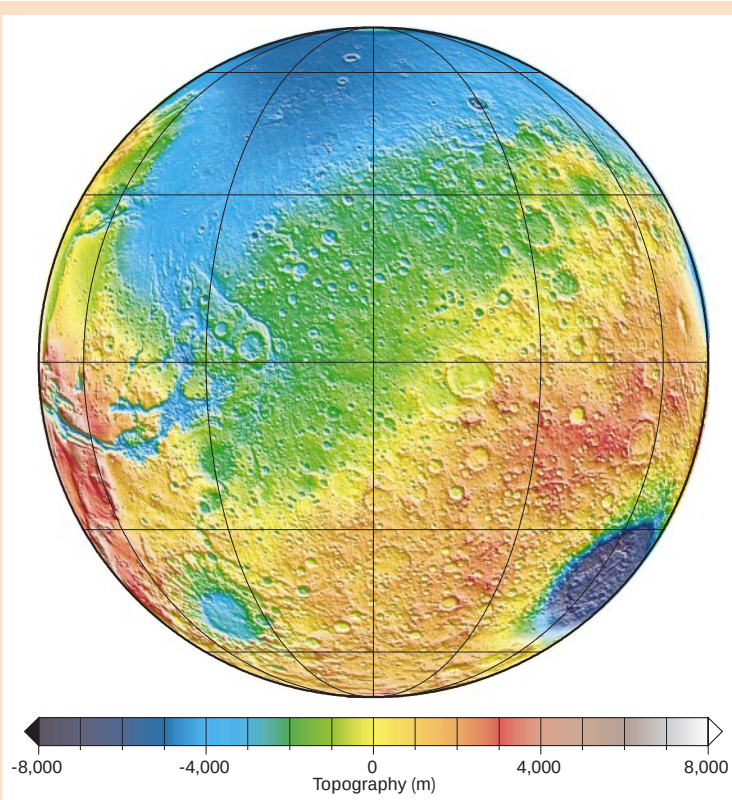

Figure 5 Spherical projection of Mars' topography[54] with 0° E longitude at front centre. The Hellas impact basin is located at the lower-right edge, with the low elevation of the basement depression shown in purple. The figure highlights the 2-km-high annulus of material that surrounds the basin and contributes to the elevation difference between Mars' southern and northern hemispheres.

The age of basement crust beneath the resurfaced northern plains and the timing of the resurfacing are key factors in understanding Mars' geological evolution. The buried Utopia basin demands that the crust beneath the northern plains is Noachian in age, as impactors of the required size would have been swept up by the planets shortly after accretion. Obscured and partially buried craters provide additional evidence for the age of the northern lowlands and the sequence of events in its history. The size–frequency distribution of topographic arcs resembling crater rims and large, shallow circular depressions[68] indicates that the number of craters beneath the northern plains is comparable to that in the southern highlands. Thus the northern lowlands beneath the later plains material are approximately as old as southern highlands — that is, Noachian in age.

Because crater diameter scales with depth[70], the relief of partially buried craters can be used to estimate the thickness of lowland fill. Recent analysis using this approach shows that the northern plains vary spatially in thickness[68]. The density of partially buried craters within the much larger and deeper Utopia basin dictates that at least some of the resurfacing occurred not long after the formation of Utopia; if such craters had accumulated on the original floor of Utopia, the fill is sufficiently thick that they would not be detectable. It seems likely that much of the fill in Utopia consists of sediments transported from the southern highlands during the Noachian, when

water flowed freely on the surface (ref. 71, and see review in this issue by Leovy, pages 245–249). Massive erosion in the southern highlands[72] may have been driven by volatiles associated with the formation of Tharsis in the Noachian[73]. The deep fill in Utopia may contain material that eroded from the southern highlands, forming the dichotomy boundary scarp, which is developed prominently south of Utopia[74]. These observations place important constraints on geological evolution models: any explanation for the northern lowlands must now explain both the low elevation and infilling, and the realization that these events occurred at different times.

Many impact craters on Mars have unusual ejecta blankets referred to as 'ramparts' (Fig. 4), which have been interpreted as evidence for impact into a water- or ice-rich substrate. Recent analysis of high-resolution Mars topography[54,75] has shown that virtually all impact craters on the northern plains larger than about 3 km in diameter display rampart structures, which provides evidence that ice or water was ubiquitous in the subsurface of the northern hemisphere during the Hesperian epoch and possibly more recent times.

Mantle dynamics and thermal evolution

Lithosphere and heat flow

Models of the thermal evolution of Mars are sensitive to the distribution of internal heat sources and the style of mantle heat loss, which depends on internal structure and temperature distribution[76]. Models of heat loss by thermal convection require assumptions about the concentrations of radioactive heat-producing elements (potassium, uranium and thorium) partitioned into the crust. These concentrations are controlled by the manner in which such large atoms partition into melt, as well as the fraction of the mantle that melted to generate the crust[77].

Joint analysis of gravity and topography has yielded estimates of the effective elastic thickness of the martian lithosphere (the outer shell of long-term strength). The elastic thickness is usually interpreted as the depth to an isotherm (~650 °C) beneath which the martian interior is too weak to support stresses over geologically long (~10^8 year) intervals. Measures of elastic thickness allow estimates of surface heat flow, which provide constraints on models of thermal evolution. Results reveal a significant variability in lithosphere structure among the main crustal provinces[53,78], but show a general trend: elastic thickness values generally decrease with increasing surface age, consistent with declining heat flux from the martian mantle with time. The southern highlands are oldest, indicative of crustal stabilization earliest in martian history, followed by the northern lowlands, which display an elastic thickness that reflects the thermal state during the period of northern-hemisphere resurfacing. Although Tharsis as a whole is old, it displays the thickest lithosphere, with implied heat flow reflecting the thermal state during the formation of the volcanoes, which formed relatively recently in comparison to the ancient and broad rise[46].

Thermal evolution

Thermal evolution models[39,79,80], constructed for a range of geometries, initial conditions, mantle viscosity structures and heat-production scenarios, all indicate a significantly declining heat flow with time. Uniform viscosity models[39] produce the slowest cooling during early martian evolution, whereas models with strongly temperature-dependent viscosity[80–82] show the most rapid fall-off in early heat flow.

Sleep[1] has suggested that plate tectonics operated during the Noachian epoch and that the northern-hemisphere crust formed by crustal spreading. His model predicted a specific plate configuration that included active and passive margins, the latter of which correlate with the geological expression of the dichotomy. Although no obvious geophysical signature of the hypothesized long-extinct margins is preserved, it may be possible to test the hypothesis more specifically with recently acquired data. A northern-lowlands crust of thickness ~35 km (Fig. 2) could be produced by crustal spreading if the mantle temperature were somewhat greater than that typical of modern terrestrial mid-ocean ridges[83]. However, it is unclear whether a such a thick crust could subduct and drive plate recycling, because the basalt–eclogite phase transition, which aids subduction, would not occur on Mars until a depth of ~200 km.

Box 1
Martian geological timescale

The martian geological record is inferred on the basis of mapped stratigraphy[123]. Relative ages of stratigraphic units are based on superposition relationships. Absolute numerical ages can be assigned given models that relate the estimated impact-crater flux to the areal density of craters on distinct parts of the planetary surface. In discussing geological time, 1 Gyr is 10^9 years and 1 Myr is 10^6 years. The figure shows the martian stratigraphic epochs from oldest to youngest: the Noachian, Hesperian and Amazonian. Along with the stratigraphic record is a recent estimate of the absolute timescale[124].

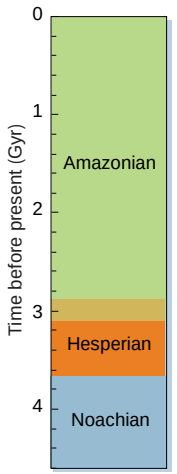

Formation of Tharsis

Various studies have used fault patterns and gravity/topography relationships[84–88] in an attempt to understand the formation of Tharsis. As contributors to the formation of the province, data and models suggest a combination of volcanic construction and uplift, and heating associated with a major mantle plume or plumes. The presence or absence of a lower-mantle perovskite layer has significant implications for development of a hemispheric-scale plume. Convection in a martian mantle that contains the spinel-to-perovskite phase transition[89–93] will suppress short-wavelength convective perturbations and preferentially develop long-wavelength flow. The velocity field may form a single upwelling plume that could potentially explain the formation of Tharsis, although models have not yet produced the desired pattern in sufficiently short timescales. A single thermal plume could provide the heat source required for extensive magmatism and volcanism, and could account for a fraction of the topographic uplift of Tharsis, although most of the current topography is probably due to piling up of volcanic material[53,63,94].

The location of Tharsis as antipodal to the Hellas impact basins has raised the suggestion that the impact could have initiated the mantle thermal anomaly that led to Tharsis. However, no model has demonstrated the plausibility of this idea. The location of Tharsis on the boundary of the northern and southern crustal-thickness provinces might not be coincidental. Models of continent–ocean boundaries on Earth[95] show a focusing of convective activity.

Formation of the crustal dichotomy

Hypotheses to explain the hemispheric dichotomy have included one or more massive impacts into the northern hemisphere[96,97], thinning of the northern-hemisphere crust by mantle convection[98–100], and an early period of tectonic-plate recycling[1]. No assessments before MGS[74,101] took into account the difference between the dichotomy as expressed in the surface geology and topography and that apparent in the crustal structure. Topography and crustal-structure data pose three challenges for impact-origin hypotheses, the first being the lack of global correlation of crustal thickness with the geological expression of the dichotomy (Fig. 2). Second, the topography (Fig. 4) and crustal thickness reveal a distinctly non-circular outline of the

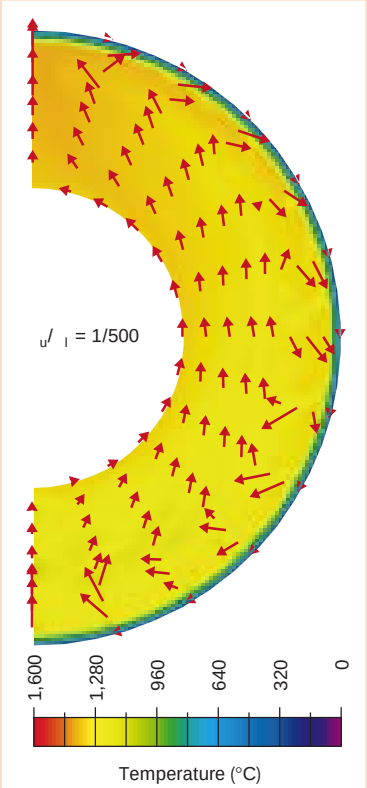

Figure 6 Convection calculation illustrating concentration of heat loss in one hemisphere of Mars. The calculation uses a finite element approach and assumes axisymmetric geometry[122]. The figure shows temperature (in colour) and velocity (arrows) fields for a martian mantle with a 750-km-thick low-viscosity upper layer. The model is characterized by an 80-km-thick conductive lid, a viscosity contrast between the upper and lower mantle layers of 1/500, and a core size of half the planetary radius. Free slip and isothermal boundary conditions were imposed at the surface and crust–mantle boundary. The calculation includes internal heat production and temperature- and depth-dependent viscosity. The convection pattern results in preferential heating of one hemisphere that could potentially explain the dichotomy in crustal structure.

northern lowlands that cannot be explained easily by one or a few large impacts. And third, circular zones of crustal thinning that are characteristic of large impact basins are not apparent other than for Utopia. If the northern depression formed as a result of impact, it must have occurred very early in martian history (that is, before the formation of Utopia), and the topographic and crustal-thickness signatures must have been modified by subsequent processes.

A surprising result from MGS is that the geological expression of the dichotomy may be due in part to an impact in the southern hemisphere. Figure 5 illustrates the concentric nature of material around Hellas, which plausibly has been excavated during impact. The annulus stands 2 km above its surroundings and accounts for a significant amount of the high-standing topography of the southern hemisphere. Material excavated from Hellas represents a major re-distribution of the martian crust[53], contributing in part to the surficial expression of topography along part of the dichotomy boundary[45]. However, Hellas' contribution to the geological dichotomy does not explain all the elevated topography in the southern hemisphere, nor does it account for the geological contrast between the hemispheres and the presence of a scarp at some parts of the boundary.

Mantle convection models for the origin of the dichotomy require a long-wavelength pattern of heat loss with upwelling in one hemisphere and downwelling in the other. Convective mechanisms have also been problematic because although hemispheric-scale mantle-flow models have been developed for the Moon[102], it has been difficult to produce a long-wavelength pattern of heat loss in a planet with a core as large as Mars has[39,103]. The reason for the difficulty has been the assumption that the mantle is of uniform viscosity. Hemispheric-scale convection is possible if, as for Earth, the martian mantle is layered in viscosity such that the upper mantle is at least 100 times less viscous than the lower mantle (Fig. 6). Such a layer could correspond to a martian asthenosphere, as occurs on Earth beneath the lithosphere. As the viscosity of the lower layer increases relative to the upper layer, deformation becomes more efficient at longer wavelengths. For conditions that may be plausible for early Mars, a hemispheric pattern of heat loss develops in about 230 Myr and is maintained for over 1 Gyr, and could potentially explain early formation of crust in the Noachian as well as volcanic resurfacing of the northern lowlands in the Hesperian. A long-wavelength convective pattern cools the core and mantle more efficiently than shorter-wavelength convection and could have contributed to the demise of the core dynamo (ref. 104, and see review in this issue by Stevenson, pages 214–219).

Crustal magnetization

Vector magnetic-field measurements from MGS[105–107] reveal broad, intense zones of alternating magnetic polarity in the southern-hemisphere crust (Terra Cimmeria) and several isolated anomalies in the northern lowlands (Fig. 1 in the review by Stevenson). The radial components of the anomalies have amplitudes an order of magnitude or more greater than anomalies on Earth measured at comparable altitude[108]. On Earth, continental magnetic anomalies are thought to be mostly due to magnetic induction by the Earth's dipole field, whereas the oceanic crust displays magnetic stripes dominated by remanence. At present, Mars lacks an internally generated dipole magnetic field, and crustal anomalies most likely represent remanent magnetism from an internal field in the distant past[105,109]. Stevenson (pages 214–219) presents evidence for a vigorous core dynamo that operated during the Noachian, before the end of heavy bombardment. Here we focus on the nature of crustal magnetization and its relationship to crustal formation.

The magnetic properties of crustal rocks are determined by their iron mineralogy[110], which bears on crustal composition as well as formation or alteration conditions. The intensity of observed magnetizations on Mars implies that the magnetizing process is probably thermoremanence, which is more efficient at magnetizing rocks than remanence associated with crystallization or sediment deposition. The minerals responsible for intense magnetization of the martian crust are likely to be similar to the most magnetizing constituents in Earth's crust[111,112], with the martian examples characterized by higher average iron abundances. Favoured are minerals with high magnetic remanence, such as pyrrhotite (Fe_7S_8), magnetite (Fe_3O_4), titanomagnetite (Fe_2O_3-$FeTiO_3$), haematite (Fe_2O_3) and magheamite (γ-Fe_2O_3). Most of these minerals have been detected from MGS orbital spectroscopy[113], lander surface analysis[114] or martian meteorites[115,116]. Their existence suggests a more oxidizing environment than that which characterizes the martian mantle[38], which suggests that aqueous alteration might have contributed to magnetization[17,37].

The timing of magnetization is related to the nature of crustal formation. The concentration of magnetization in southern-hemisphere crust and the absence of anomalies in the Hellas basin points to the early operation and subsequent demise of a dynamo early in martian history, implying rapid cooling of the crust (refs 105, 109, and the review by Stevenson). Magnetization of martian meteorite ALH84001 (ref. 116) is also consistent with an early dynamo. An alternative suggestion — that the dynamo turned on later in martian history[117] — requires magmatic additions to, or thermal re-working of, the crust. Figure 2 shows that the crustal structure of the magnetized region in Terra Cimmeria does not seem to be distinctive from the non-magnetized parts of the southern hemisphere. There is no apparent evidence from the crustal structure for proposed intrusive magmatism, although such evidence is apparent in the Tharsis and Elysium regions. If there were later-stage intrusions or re-working of southern-hemisphere crust, the evidence must be at smaller spatial scales than the resolution of the crustal thickness model. The existence of localized magnetic anomalies in the northern lowlands and part of Tharsis, which display surface ages that range from Hesperian to Amazonian, has been invoked as additional evidence of a late turn-on of the martian dynamo[117]. But these anomalies do not correlate with surface topography and must be a consequence of buried sources[52,53], perhaps impacts, of likely Noachian age[68].

On the basis of amplitudes of magnetic anomalies and assuming a magnetic intensity comparable to that of Earth's upper oceanic crust[110], the depth of the so-called Curie temperature for magnetization in Terra Cimmeria is the same as the thickness of the elastic lithosphere (~30 km)[53,78]. Thus magnetics, gravity and topography provide similar estimates of the thermal state of the southern-hemisphere crust at the time of thermal stabilization.

Formation and evolution of the crust

Analysis of tungsten isotopes suggests that the martian core formed within the first 30 Myr of Solar System history[118]. The tungsten anomalies, which are controlled by metal-silicate fractionation and thus date core formation, correlate with neodymium anomalies, which are controlled by the formation of silicate magmas, and thus probably date mantle differentiation to form the crust. This correlation argues that core and crust formation were probably close to synchronous. These data also suggest that Mars has not experienced any significant large-scale convective mixing of the mantle or impact re-distribution of the crust since the time of core formation. However, it is difficult to reconcile this latter result with the evidence for a rapidly cooling (and therefore dynamically mixing) early mantle.

It has been suggested that, like the Earth's moon, primordial Mars was characterized by a 'magma ocean'[119] that cooled to form the crust. But although limited possible evidence has been cited on the basis of isotopic signatures of the shergottites[120], surface geochemical evidence for such a phenomenon has not yet been identified. If Mars exhibited an early period of pervasive shallow melting, the thermal and compositional layering that would have resulted could have suppressed convective cooling of the mantle. It might also have allowed conductive cooling to significantly reduce temperatures at the base of the crust, allowing variations in crustal thickness to be preserved for a longer time.

Unsolved questions

Analyses of martian meteorites and the wealth of orbital data from MGS have greatly aided our understanding of the chemistry and structure of the martian crust and mantle, but many fundamental questions remain. What was the mechanism of crustal formation, and how is it related to planetary differentiation and the formation of the crustal dichotomy? Did the crust form with a structure similar to that currently observed, or did it develop more uniformly and evolve to the present configuration? How is the mantle stratified in mineralogy and viscosity? What is the temporal evolution of mantle dynamics and why did the planet cool so fast so early? Is there a causal relationship between Tharsis and the hemispheric dichotomy? What is the nature of highly magnetized crustal materials? Where are the carbonate and sulphate deposits that were expected to have formed in Mars' earlier, wetter environment? And what was the inventory and role of water in the geophysical, geological and climatological evolution of Mars? Progress on these questions can be attained by a well-balanced programme of theoretical and experimental investigations (see article in this issue by Carr and Garvin, pages 250–253), spacecraft exploration that includes orbiters, low-altitude platforms and *in situ* observations, and analysis of samples of the martian crust returned to Earth. □

1. Sleep, N. H. Martian plate tectonics. *J. Geophys. Res.* **99,** 5639–5655 (1994).
2. Bell, J. F. I. *et al.* Near-infrared imaging of Mars from HST: surface reflectance, photometric properties, and implications for MOLA data. *Icarus* **138,** 25–35 (1999).
3. Soderblom, L. A. in *Mars* (eds Kieffer, H. H., Jakosky, B. M., Snyder, C. W. & Matthews, M. S.) 557–593 (Univ. Arizona Press, Tucson, 1992).
4. Mustard, J. F. *et al.* The surface of Syrtis Major: composition of the volcanic substrate and mixing with altered dust and soil. *J. Geophys. Res.* **98,** 3387–3400 (1993).
5. Mustard, J. F. & Sunshine, J. M. Seeing through the dust: Martian crustal heterogeneity and links to the SNC meteorites. *Science* **267,** 1623–1626 (1995).
6. Bandfield, J. L., Hamilton, V. E. & Christensen, P. R. A global view of Martian surface composition from MGS-TES. *Science* **287,** 1626–1630 (2000).
7. McSween, H. Y. *et al.* Chemical, multispectral, and textural constraints on the composition and origin of rocks at the Mars Pathfinder site. *J. Geophys. Res.* **104,** 8679–8715 (1999).
8. McSween, H. Y. Jr SNC meteorites: clues to Martian petrologic evolution? *Rev. Geophys.* **23,** 391–416 (1985).
9. McSween, H. Y. Jr What have we learned about Mars from SNC meteorites? *Meteoritics* **29,** 757–779 (1994).
10. Sherman, D. M., Burns, R. G. & Burns, V., M. Spectral characteristics of the iron oxides with application to the Martian bright region mineralogy. *J. Geophys. Res.* **87,** 10169–10180 (1982).
11. Bell, J. F. in *Mineral Spectroscopy: A Tribute to Roger G. Burns* (eds Dyan, M. D., McCammon, C. & Schaefer, M. W.) (Geol. Soc. Spec. Pub. 5) 359–380 (Geol. Soc., Boulder, 1996).
12. Fanale, F. P., Postawko, S. E., Pollack, J. B., Carr, M. H. & Pepin, R. O. in *Mars* (eds Kieffer, H. H., Jakosky, B. M., Snyder, C. W. & Matthews, M. S.) 1135–1179 (Univ. Arizona Press, Tucson, 1992).
13. Morris, R. V. *et al.* Mineralogy, composition, and alteration of Mars Pathfinder rocks and soils: evidence from multispectral, elemental, and magnetic data on terrestrial analogue, SNC meteorite, and Pathfinder samples. *J. Geophys. Res.* **105,** 1757–1817 (2000).
14. Christensen, P. C., Bandfield, J. L., Smith, M. D., Hamilton, V. E. & Clark, R. N. Identification of a basaltic component of the Martian surface from Thermal Emission Spectrometer data. *J. Geophys. Res.* **105,** 9609–9621 (2000).
15. Christensen, P. R. *et al.* The Mars Global Surveyor Thermal Emission Spectrometer experiment: investigation description and surface science. *J. Geophys. Res.* (in the press).
16. Minitti, M. E. & Rutherford, M. J. Genesis of the Mars Pathfinder "sulfur-free" rock from SNC parental liquids. *Geochim. Cosmochim. Acta* **64,** 2535–2547 (2000).
17. McSween, H. Y. Jr *et al.* Geochemical evidence for magmatic water within Mars from pyroxenes in the Shergotty meteorite. *Nature* **409,** 487–490 (2001).
18. Noble, S. K. & Pieters, C. M. Type 2 terrain: compositional constraints on the Martian lowlands. Lunar Planet. Sci. Conf. XXXII, Abstr. 1230 <http://www.lpi.usra.edu/meetings/lpsc2001/pdf/1230.pdf> (2001).
19. Jagoutz, E. Chronology of SNC meteorites. *Space Sci. Rev.* **56,** 13–22 (1991).
20. Chen, J. H. & Wasserburg, G. J. Formation ages and evolution of Shergotty and its parent planet from U-Th-Pb systematics. *Geochim. Cosmochim. Acta* **50,** 955–968 (1986).
21. Borg, L. E., Nyquist, L. E., Taylor, L. A., Weisman, H. & Shih, C.-Y. Constraints on Martian differentiation processes from Rb-Sr and Sm-Nd isotopic analyses of the basaltic shergottite QUE94201. *Geochim. Cosmochim. Acta* **61,** 4915–4931 (1997).
22. Bogard, D. D. & Johnson, P. Noble gases in the antarctic meteorite. *Science* **221,** 651–654 (1983).
23. Bogard, D. D., Nyquist, L. E. & Johnson, P. Noble gas contents of shergottites and implications for the Martian origin of SNC meteorites. *Geochim. Cosmochim. Acta* **48,** 1723–1739 (1984).
24. Swindle, T. D., Caffee, M. W. & Hohenberg, C. M. Xenon and other noble gases in shergottites. *Geochim. Cosmochim. Acta* **50,** 1001–1015 (1986).
25. Wiens, R. C., Becker, R. H. & Pepin, R. O. The case for a martian origin of the shergottites. II. Trapped and indigenous gas components in EETA79001 glass. *Earth Planet. Sci. Lett.* **77,** 149–158 (1986).
26. McKay, D. S. *et al.* Search for past life on Mars: possible relic biogenic activity in Martian meteorite ALH84001. *Science* **273,** 924–930 (1996).
27. Mittlefeldt, D. W. ALH84001, a cumulate orthopyroxenite member of the martian meteorite clan. *Meteoritics* **29,** 214–221 (1994).
28. Ash, R. D., Knott, S. F. & Turner, G. A 4-Gyr shock age for a martian meteorite and implications for the cratering history of Mars. *Nature* **380,** 57–59 (1996).
29. Treiman, A. H. A petrographic history of Martian meteorite ALH84001: two shocks and an ancient age. *Meteoritics* **30,** 294–302 (1995).
30. Treiman, A. H. The history of Allan Hills 84001 revised: multiple shock events. *Meteoritics Planet. Sci.* **33,** 753–764 (1998).
31. Wood, J. A. *et al.* in *Basaltic Volcanism on the Terrestrial Planets* (eds McGetchin, T. R., Pepin, R. O. & Phillips, R. J.) 634–699 (Pergamon, New York, 1981).
32. Bills, B. G. Geodetic constraints on the composition of Mars. *J. Geophys. Res.* **95,** 14131–14136 (1990).
33. Folkner, W. M., Yoder, C. F., Yuan, D. N., Standish, E. M. & Preston, R. A. Interior structure and seasonal mass redistribution of Mars from radio tracking of Mars Pathfinder. *Science* **278,** 1749–1752 (1997).
34. Dreibus, G. & Wanke, H. Mars: a volatile-rich planet. *Meteoritics* **20,** 367–382 (1985).
35. Longhi, J., Knittle, E., Holloway, J. R. & Wanke, H. in *Mars* (eds Kieffer, H. H., Jakosky, B. M., Snyder, C. W. & Matthews, M. S.) 184–208 (Univ. Arizona Press, Tucson, 1992).
36. Bertka, C. M. & Fei, Y. Implications of Mars Pathfinder data for the accretion history of the terrestrial planets. *Science* **281,** 1838–1840 (1998).
37. Wadhwa, M. Redox state of Mars' upper mantle and crust from Eu anomalies in shergottite pyroxenes. *Science* **291,** 1527–1530 (2001).
38. Wanke, H. & Dreibus, G. Chemical composition and accretion history of the terrestrial planets. *Phil. Trans. R. Soc. Lond. A* **325,** 545–557 (1988).
39. Schubert, G. & Spohn, T. Thermal history of Mars and the sulfur content of its core. *J. Geophys. Res.* **95,** 14095–14104 (1990).
40. Tanaka, K. L., Scott, D. H. & Greeley, R. in *Mars* (eds Kieffer, H. H., Jakosky, B. M., Snyder, C. W. & Matthews, M. S.) 345–382 (Univ. Arizona Press, Tucson, 1992).
41. Solomon, S. C. *et al.* What happened when on Mars? Some insights into the timing of major events from Mars Global Surveyor data. *EOS Trans. Am. Geophys. Union* P31A-06 (2001).
42. Mutch, T. A., Arvidson, R. E., Head, J. W., Jones, K. L. & Saunders, R. S. *The Geology of Mars* (Princeton Univ. Press, Princeton, 1976).
43. Carr, M. H. *The Surface of Mars* (Yale Univ. Press, New Haven, 1981).
44. Smith, D. E. & Zuber, M. T. The shape of Mars and the topographic signature of the hemispheric dichotomy. *Science* **271,** 184–188 (1996).
45. Smith, D. E. *et al.* The global topography of Mars and implications for surface evolution. *Science* **284,** 1495–1503 (1999).
46. Scott, D. H. & Tanaka, K. L. Geologic map of the western equatorial region of Mars. US Geol. Survey Map I-1802-A (1986).
47. Greeley, R. & Guest, J. E. Geologic map of the eastern equatorial region of Mars. US Geol. Survey Map I-1802-B (1987).
48. Sharp, R. P., Soderblom, L. A., Murray, B. C. & Cutts, J. A. The surface of Mars 2. Uncratered terrains. *J. Geophys. Res.* **76,** 331–342 (1971).
49. Sharp, R. P. Mars: fretted and chaotic terrains. *J. Geophys. Res.* **78,** 4073–4083 (1973).
50. Frey, H., Sakimoto, S. E. & Roark, J. The MOLA topographic signature at the crustal dichotomy boundary. *Geophys. Res. Lett.* **25,** 4409–4412 (1998).

51. McGill, G. E. Buried topography of Utopia, Mars: persistence of a giant impact depression. *J. Geophys. Res.* **94,** 2753–2759 (1989).
52. Smith, D. E. *et al.* The gravity field of Mars: results from Mars Global Surveyor. *Science* **286,** 94–97 (1999).
53. Zuber, M. T. *et al.* Internal structure and early thermal evolution of Mars from Mars Global Surveyor topography and gravity. *Science* **287,** 1788–1793 (2000).
54. Smith, D. E. *et al.* Mars Orbiter Laser Altimeter (MOLA): experiment summary after the first year of global mapping of Mars. *J. Geophys. Res.* (in the press).
55. Lemoine, F. G. *et al.* An improved solution of the gravity field of Mars (GMM-2B) from Mars Global Surveyor. *J. Geophys. Res.* (in the press).
56. Albee, A. A., Palluconi, F. D. & Arvidson, R. E. Mars Global Surveyor mission: overview and status. *Science* **279,** 1671–1672 (1998).
57. Nimmo, F. & Stevenson, D. Estimates of Martian crustal thickness from viscous relaxation of topography. *J. Geophys. Res.* **106,** 5085–5098 (2001).
58. Sohl, F. & Spohn, T. The interior structure of Mars: implications from SNC meteorites. *J. Geophys. Res.* **102,** 1613–1635 (1997).
59. Janle, P. Bouguer gravity profiles across the highland-lowland escarpment on Mars. *Earth, Moon Planets* **28,** 55–67 (1983).
60. Spohn, T., Sohl, F. & Breuer, D. Mars. *Astron. Astrophys. Rev.* **8,** 181–236 (1998).
61. Bratt, S. R., Solomon, S. C., Head, J. W. & Thurber, C. H. The deep structure of lunar basins: implications for basin formation and modification. *J. Geophys. Res.* **90,** 3049–3064 (1985).
62. Zuber, M. T., Smith, D. E., Lemoine, F. G. & Neumann, G. A. The shape and internal structure of the Moon from the Clementine mission. *Science* **266,** 1839–1843 (1994).
63. Solomon, S. C. & Head, J. W. Evolution of the Tharsis province of Mars: the importance of heterogeneous lithospheric thickness and volcanic construction. *J. Geophys. Res.* **82,** 9755–9774 (1982).
64. McEwen, A. S., Malin, M. C., Carr, M. H. & Hartmann, W. K. Voluminous volcanism on early Mars revealed in Valles Marineris. *Nature* **397,** 584–586 (1999).
65. Greeley, R. & Spudis, P. D. Volcanism on Mars. *Rev. Geophys.* **19,** 13–41 (1981).
66. Head, J. W., Kreslavsky, M. A. & Pratt, S. Northern lowlands of Mars: evidence for widespread volcanic flooding and tectonic deformation in the Hesperian period. *J. Geophys. Res.* (in the press).
67. Withers, P. & Neumann, G. A. Enigmatic northern plains of Mars. *Nature* **410,** 651 (2001).
68. Frey, H., Shockey, K. M., Frey, E. L., Roark, J. H. & Sakimoto, S. E. H. A very large population of likely buried impact basins in the northern lowlands of Mars revealed by MOLA data. Lunar Planet. Sci. Conf. XXXII, Abstr. 1680 <http://www.lpi.usra.edu/meetings/lpsc2001/pdf/1680.pdf> (2001).
69. Kreslavsky, M. A. & Head, J. W. III Stealth craters in the northern lowlands of Mars: evidence for a buried Early-Hesperian-aged unit. Lunar Planet. Sci. Conf. XXXII, Abstr. 1001 <http://www.lpi.usra.edu/meetings/lpsc2001/pdf/1001.pdf> (2001).
70. Pike, R. J. Depth/diameter relations of fresh lunar craters: revision from spacecraft data. *Geophys. Res. Lett.* **1,** 291–294 (1974).
71. Squyres, S. W. & Kasting, J. F. Early Mars: how warm and how wet? *Science* **265,** 744–749 (1994).
72. Hynek, B. M. & Phillips, R. J. Evidence for extensive denudation of the Martian highlands. *Geology* **29,** 407–410 (2001).
73. Phillips, R. J. *et al.* Ancient geodynamics and global-scale hydrology on Mars. *Science* **291,** 2587–2591 (2001).
74. McGill, G. E. & Dimitriou, A. M. Origin of the Martian global dichotomy by crustal thinning in the late Noachian or early Hesperian. *J. Geophys. Res.* **95,** 12595–12605 (1990).
75. Garvin, J. B. & Frawley, J. J. Geometric properties of Martian impact craters: preliminary results from the Mars Orbiter Laser Altimeter. *Geophys. Res. Lett.* **25,** 4405–4408 (1998).
76. Sleep, N. H. Evolution of the mode of convection within terrestrial planets. *J. Geophys. Res.* **105,** 17563–17578 (2000).
77. Parmentier, E. M. & Zuber, M. T. Relaxation of crustal thickness variations on Mars: implications for thermal evolution. Lunar Planet. Sci. Conf. XXXII, Abstr. 1357 <http://www.lpi.usra.edu/meetings/lpsc2001/pdf/1357.pdf> (2001).
78. McGovern, P. J. *et al.* Gravity/topography admittances and lithospheric evolution of Mars: the importance of finite-amplitude topography. Lunar Planet. Sci. Conf. XXXII, Abstr. 1804 <http://www.lpi.usra.edu/meetings/lpsc2001/pdf/1804.pdf> (2001).
79. Schubert, G., Solomon, S. C., Turcotte, D. L., Drake, M. J. & Sleep, N. H. in *Mars* (eds Kieffer, H. H., Jakosky, B. M., Snyder, C. W. & Matthews, M. S.) 147–183 (Univ. Arizona Press, Tucson, 1992).
80. Grasset, O. & Parmentier, E. M. Thermal convection in a volumetrically heated, infinite Prandtl number fluid with strongly temperature-dependent viscosity: implications for planetary thermal evolution. *J. Geophys. Res.* **103,** 18171–18181 (1998).
81. Choblet, G., Grasset, O., Parmentier, E. M. & Sotin, C. Mars thermal evolution revisited. Lunar Planet. Sci. Conf. XXX, Abstr. 1556 <http://www.lpi.usra.edu/meetings/LPSC99/pdf/1556.pdf> (1999).
82. Spohn, T. Thermal histories of the terrestrial planets revisited. *EOS Trans. Am. Geophys. Union* **80,** P32B-05 (1999).
83. Forsyth, D. W. Crustal thickness and the average depth and degree of melting in fractional melting models of passive flow beneath mid-ocean ridges. *J. Geophys. Res.* **98,** 16073–16079 (1993).
84. Banerdt, W. B., Phillips, R. J., Sleep, N. H. & Saunders, R. S. Thick shell tectonics on one-plate planets: applications to Mars. *J. Geophys. Res.* **87,** 9723–9733 (1982).
85. Banerdt, W. B., Golombek, M. P. & Tanaka, K. L. in *Mars* (eds Kieffer, H. H., Jakosky, B. M., Snyder, C. W. & Matthews, M. S.) 249–297 (Univ. Arizona Press, Tucson, 1992).
86. Bills, B. G. & Nerem, R. S. A harmonic analysis of Martian topography. *J. Geophys. Res.* **100,** 26314–26326 (1995).
87. Harder, H. Mantle convection and the dynamic geoid of Mars. *Geophys. Res. Lett.* **27,** 301–304 (2000).
88. Anderson, R. C. & Golombek, M. P. Timing of Tharsis uplift from the distribution of tectonic structures. *J. Geophys. Res.* (in the press).
89. Weinstein, S. A. The effects of a deep mantle endothermic phase transition. *J. Geophys. Res.* **100,** 11719–11728 (1995).
90. Harder, H. & Christensen, U. A one-plume model of Martian mantle convection. *Nature* **380,** 507–509 (1996).
91. Breuer, D., Zhou, H., Yuen, D. A. & Spohn, T. Phase transitions in the Martian mantle: implications for the planet's volcanic evolution. *J. Geophys. Res.* **101,** 7531–7542 (1996).
92. Breuer, D., Yuen, D. A. & Spohn, T. Phase transitions in the Martian mantle: implications for partially layered convection. *Earth Planet. Sci. Lett.* **148,** 457–469 (1997).
93. Breuer, D., Yuen, D. A., Spohn, T. & Zhang, S. Three-dimensional models of Martian mantle convection with phase transitions. *Geophys. Res. Lett.* **25,** 229–232 (1998).
94. Zhong, S. Long-wavelength topography and gravity anomalies of Mars and their implications to the formation of the Tharsis rise. Lunar Planet. Sci. Conf. XXXII, Abstr. 2124 <http://www.lpi.usra.edu/meetings/lpsc2001/pdf/2124.pdf> (2001).
95. King, S. D. & Ritsema, J. African hot spot volcanism: small-scale convection in the upper mantle beneath cratons. *Science* **290,** 1137–1140 (2000).
96. Wilhelms, D. E. & Squyres, S. W. The Martian hemispheric dichotomy may be due to a giant impact. *Nature* **309,** 138–140 (1984).
97. Frey, H. V. & Schultz, R. A. Large impact basins and the mega-impact origin for the crustal dichotomy on Mars. *Geophys. Res. Lett.* **15,** 229–232 (1988).
98. Lingenfelter, R. E. & Schubert, G. Evidence for convection in planetary interiors from first-order topography. *Moon* **7,** 172–180 (1973).
99. Wise, D. U., Golombek, M. P. & McGill, G. E. Tectonic evolution of Mars. *J. Geophys. Res.* **84,** 7934–7939 (1979).
100. Wise, D. U., Golombek, M. P. & McGill, G. E. Tharsis province of Mars: geologic sequence, geometry, and a deformation mechanism. *Icarus* **35,** 456–472 (1979).
101. McGill, G. E. & Squyres, S. W. Origin of the Martian crustal dichotomy: evaluating hypotheses. *Icarus* **93,** 386–393 (1991).
102. Zhong, S., Parmentier, E. M. & Zuber, M. T. On the dynamic origin and asymmetric distribution of mare basalts. *Earth Planet. Sci. Lett.* **177,** 131–141 (2000).
103. Schubert, G., Bercovici, D. & Glatzmaier, G. A. Mantle dynamics in Mars and Venus: influence of an immobile lithosphere on three-dimensional mantle convection. *J. Geophys. Res.* **94,** 14105–14129 (1990).
104. Nimmo, F. & Stevenson, D. J. Influence of early plate tectonics on the thermal evolution and magnetic field of Mars. *J. Geophys. Res.* **105,** 11969–11979 (2000).
105. Acuna, M. H. *et al.* Global distribution of crustal magnetization discovered by the Mars Global Surveyor MAG/ER experiment. *Science* **284,** 790–793 (1999).
106. Connerney, J. E. P. *et al.* Magnetic lineations in the ancient crust of Mars. *Science* **284,** 794–798 (1999).
107. Purucker, M. *et al.* An altitude-normalized magnetic map of Mars and its interpretation. *Geophys. Res. Lett.* **27,** 2449–2452 (2000).
108. Langel, R. A., Phillips, J. D. & Horner, R. J. Initial vector magnetic anomaly map from MAGSAT. *Geophys. Res. Lett.* **9,** 269–272 (1982).
109. Acuna, M. H. *et al.* Results of the Mars Global Surveyor magnetic field investigation. *J. Geophys. Res.* (in the press).
110. Dunlop, D. J. & Ozdemir, O. *Rock Magnetism* (Cambridge Univ. Press, Cambridge, 1997).
111. Kletetschka, G., Wasilewski, P. J. & Taylor, P. T. Unique thermoremanent magnetization of multidomain sized hematite: implications for magnetic anomalies. *Earth Planet. Sci. Lett.* **176,** 469–479 (2000).
112. Kletetschka, G., Wasilewski, P. J. & Taylor, P. T. Mineralogy of the sources for magnetic anomalies on Mars. *Meteoritics Planet. Sci.* **35,** 895–899 (2000).
113. Christensen, P. C. *et al.* Detection of crystalline hematite mineralization on Mars by the Thermal Emission Spectrometer: evidence for near-surface water. *J. Geophys. Res.* **105,** 9623–9642 (2000).
114. Hargraves, R. B. *et al.* Magnetic enhancement on the surface of Mars? *J. Geophys. Res.* **105,** 1819–1827 (2000).
115. Cisowski, S. M. Magnetic studies on Shergotty and other SNC meteorites. *Geochim. Cosmochim. Acta* **50,** 1043–1048 (1986).
116. Weiss, B. P., Vali, H., Baudenbacher, F. J., Stewart, S. T. & Kirschvink, J. L. Records of an ancient Martian magnetic field. *Nature* (submitted).
117. Schubert, G., Russell, C. T. & Moore, W. B. Timing of the Martian dynamo. *Nature* **408,** 666–667 (2000).
118. Lee, D.-C. & Halliday, A. N. Core formation on Mars and differentiated asteroids. *Nature* **388,** 854–857 (1997).
119. Hess, P. C. & Parmentier, E. M. Implications of magma ocean cumulate overturn for Mars. Lunar Planet. Sci. Conf. XXXII, Abstr. 1319 <http://www.lpi.usra.edu/meetings/lpsc2001/pdf/1319.pdf> (2001).
120. Blichert-Toft, J., Gleason, J. D., Telouk, P. & Albarede, F. The Lu-Hf isotope geochemistry of shergottites and the evolution of the Martian crust-mantle systems. *Earth Planet. Sci. Lett.* **173,** 25–37 (1999).
121. Neumann, G. A., Rowlands, D. S., Lemoine, F. G., Smith, D. E. & Zuber, M. T. The crossover analysis of MOLA altimetric data. *J. Geophys. Res.* (in the press).
122. Zhong, S. & Zuber, M. T. Degree-1 mantle convection and the crustal dichotomy on Mars. *Earth Planet. Sci. Lett.* 189, 75–84 (2001).
123. Tanaka, K. L. The stratigraphy of Mars. *J. Geophys. Res.* **91,** E139–E158 (1986).
124. Hartmann, W. K. & Neukum, G. Cratering chronology and the evolution of Mars. *Space Sci. Rev.* (in the press).

Acknowledgements

I thank G. Neumann and O. Aharonson for assistance with the crustal thickness inversion, H. McSween and W. Hartmann for providing material used in the figures, and J. Head, H. McSween and N. Sleep for helpful reviews. I also acknowledge helpful discussions with M. Parmentier, T. Grove, B. Weiss and members of the Mars Global Surveyor Laser Altimeter and Radio Science teams. This work was supported by the Mars Global Surveyor Project of the NASA Mars Exploration Program.